

## Influence of different cone angle of projectiles on the perforation of steel plate

### Publication History

Received: 29 April 2016

Accepted: 26 May 2016

Published: 1 July 2016

### Citation

Nand Mohan Jha, Vinod Pare, Manoj Chouksey. Influence of different cone angle of projectiles on the perforation of steel plate. *Indian Journal of Engineering*, 2016, 13(33), 331-337

# INFLUENCE OF DIFFERENT CONE ANGLE OF PROJECTILES ON THE PERFORATION OF STEEL PLATE

Nand Mohan Jha<sup>1</sup>, Vinod Pare<sup>2</sup>, Manoj Chouksey<sup>3</sup>

Mechanical Engineering Department

Shri G. S. Institute of Technology and Science Indore, 23, Park Road, Indore 452003, M.P., India

<sup>1</sup>E-mail: nmjha1991@gmail.com, <sup>2</sup>E-mail: v\_pare@yahoo.co.in, <sup>3</sup>E-mail: manoj\_chouksey@yahoo.com

## ABSTRACT

Numerical simulations with ANSYS/DYNAMIC EXPLICIT have been performed to study the Ballistic perforation of 12 mm thick Weldox 460E steel plate struck by projectiles with different cone angles (30°, 60°, 90°, 120°, 180°) under normal impact. The Johnson–Cook plasticity model combined with the Johnson–Cook dynamic failure model have been used to analyze the perforation of the target plate and the failure modes. The objective of the work was to calculate the ballistic limit, residual velocity and absorbed energy during the perforation process. Various failure modes as well as perforation process are obtained for different cone angles. Results of numerical simulation are validated with experimental results as available in literature.

**Keywords:** Cone angle, Impact velocity, Ballistic limit, Perforation

## 1. INTRODUCTION

The understanding of high velocity impact behavior of material is very important for dynamic analysis. This knowledge can be used to analyze the effect of penetrating fragment, accidental loads and collisions in various engineering application. The failure modes observed in target plate during impact by a moving projectile depends upon response of impact zone and nose shape of the projectile. Ballistic limit, which is defined as the velocity required for a particular projectile to completely penetrate a particular piece of material [1], depends on thickness of the plate and diameter of projectile.

Many investigators such as [Arias et al, Borvik et al., Zukas and scheffler, Gupta et al.] studied the dynamic behavior of material during normal impact by projectile of various nose shapes. Borvik et al. [2] found that blunt projectile took less time to perforate the target plate at low impact velocity compared to conical projectile. The amount of kinetic energy of projectile used towards the perforation of the plate depends upon the nose shape and the impact velocity. Zukas and scheffler [3] found higher ballistic limit for blunt nose projectile than conical nose projectile for thick plates experimentally. Arias et al.[4] found that blunt nosed projectile perforated the plate in less time than conical projectile. Gupta et al. [5] observed that deformation of the target plate decreases with an increase in the projectile impact velocity. Woodward [6] found that there are many cases of ballistic perforation of the plate where mixed mode of failure appears. The causes of mixed mode of failure are due to anisotropy in the material. Wilkins [7] found that ballistic limit depends on the thickness of target plate. They found that for thick metal target plate ballistic limit of blunt projectile is higher than conical projectile, while opposite was observed for thin target plate. Borvik et al. [8] found that the absorbed energy and failure modes are directly affected by the nose shape of the projectiles used during the perforation process. In present work numerical simulation has been conducted to study the effect of cone angle on perforation of metal plate by projectile during normal impact. An attempt has been made to study the influence of cone angle on failure modes, ballistic limit, absorbed energy and residual velocity. Numerical simulation has been performed in Ansys/Dynamic Explicit [9], a finite element code.

## 2. BASIC MODELLING

The plate material used in this numerical simulation of projectile-plate impact is Weldox 460 E steel. It is a thermo-mechanically rolled ferritic structural steel which offers high strength

combined with high ductility. The thermoviscoplastic behavior of the material which constitutes the metal plate has been formulated using Johnson Cook material model.

The Johnson-Cook [11] plastic model incorporate the effect of strain hardening, strain rate hardening, and thermal softening which include strain, strain rate and temperature as shown in Eq. 1.

$$\sigma(\varepsilon^p, \dot{\varepsilon}^p, T) = \left[ A + B(\varepsilon^p)^n \right] \left[ 1 + C \ln \left( \frac{\dot{\varepsilon}^p}{\dot{\varepsilon}_0} \right) \right] \left[ 1 - T^{*m} \right] \quad (1)$$

where, A is yield stress, B is constant of material, n is hardening parameter, C is strain rate sensitivity parameter, m is a temperature sensitivity parameter,  $\dot{\varepsilon}_0$  is the lower limit of constitutive relation and  $T^* = (T - T_0) / (T_m - T_0)$  is homologous temperature, T is the current temperature,  $T_0$  is the room temperature and  $T_m$  is the melting temperature in K.

The Johnson-Cook [10] dynamic failure model includes the effect of stress triaxiality, strain rate and temperature. The equivalent fracture strain is given below in Eq. 2.

$$\varepsilon_F^p = \left[ D_1 + D_2 \exp(D_3 \sigma^*) \right] \left[ 1 + D_4 \ln \frac{\varepsilon^p}{\dot{\varepsilon}_0} \right] \left[ 1 + D_5 T^* \right] \quad (2)$$

Where,  $D_i$  ( $i = 1, 2, 3, 4, 5$ ) are failure constants coefficients and  $\sigma^* = 1/3\sigma[\sigma_1 + \sigma_2 + \sigma_3]$  is stress triaxiality, which is defined as the ratio of mean stress to the equivalent stress. The model for ductile material assumes that the equivalent plastic strain at the commencement of damage is a function of stress triaxiality and strain rate. The material parameters of plate and projectile as given by Borvik et al. [2] are given in Table 1 and Table 2 respectively. The projectile behavior has been defined as elastic using a large value of the yield stress.

Table 1 material constant for weldox 460E steel

| Elastic constant and Density                |         |                             | Yield stress and strain hardening |         |                           | Strain rate hardening                    |                |                |                |
|---|---------|-----------------------------|-----------------------------------|---------|---------------------------|--|----------------|----------------|----------------|
| E (GPa)                                     | v       | $\rho$ (kg/m <sup>3</sup> ) | A (MPa)                           | B (MPa) | N                         | $\dot{\varepsilon}_0$ (s <sup>-1</sup> ) | C              |                |                |
| 200   | 0.33    | 7850                        | 490                               | 807     | 0.73                      | $5 \times 10^{-4}$                       | 0.0114         |                |                |
| Adiabatic heating and temperature softening |         |                             |                                   |         | Fracture strain constants |  |                |                |                |
| C <sub>p</sub> (J/Kg/K)                     | $\beta$ | T <sub>m</sub>              | T <sub>0</sub>                    | m       | D <sub>1</sub>            | D <sub>2</sub>                           | D <sub>3</sub> | D <sub>4</sub> | D <sub>5</sub> |
| 452   | 0.9     | 1800                        | 293                               | 0.94    | 0.0705                    | 1.732                                    | -0.54          | -0.015         | 0              |

Table 2 Material constant for projectile

| E (GPa) | v    | $\rho$ (kg/m <sup>3</sup> ) | $\sigma_y$ (MPa) | E <sub>t</sub> (MPa) | Mean $\varepsilon_f$ (%) |
|---------|------|-----------------------------|------------------|----------------------|--------------------------|
| 204     | 0.33 | 7850                        | 1900             | 15000                | 2.15                     |

### 3. NUMERICAL EXAMPLE

A numerical example for a circular plate of 500 mm diameter and 12 mm thick under normal impact by projectiles has been considered after following Borvik et al. [2]. Conical projectiles with different cone angle ( $2\theta$ ) from  $30^\circ$  to  $180^\circ$  were used for numerical analysis of projectile-plate impact as shown in Fig. 1. The mass and diameter of all projectiles were taken as 197 g and 20 mm to keep the inertial constant. The projectiles were assumed to be non-deformable.

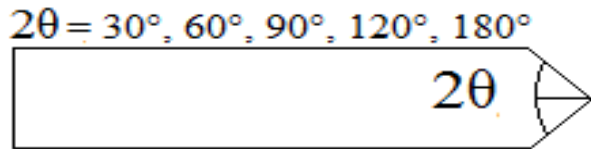


Figure 1 Projectile used for numerical analysis

Geometric configuration of the projectile and the plate was designed using Creo 5.0 [13] and imported to Ansys [9] for modeling. The target plates and projectiles were modelled using axisymmetric method. The periphery of the plate was considered as fixed for the simulation. The contact between the projectile and the plate has been defined using the penalty contact algorithm. Surface to surface contact interaction is defined between deformable steel plates and non deformable projectile with a tolerance limit of 0.2. The impact zone of the target plate is defined by  $0.2 \times 0.2 \text{ mm}^2$  element size. There are eight elements across the thickness of plate. The value of dynamic coefficient of friction is considered as 0.05 between the projectile and the target plate for the dynamic analysis.

The adaptive meshing was used for plate and projectile to avoid excessive element distortion during numerical simulation especially for smaller cone angles [9]. In case of large deformation adaptive method splits and distorts a mesh automatically during the solution process. A total of five cases of simulation with different cone angle of the projectiles are presented in the present paper. An example of finite element model is shown in Fig. 2.

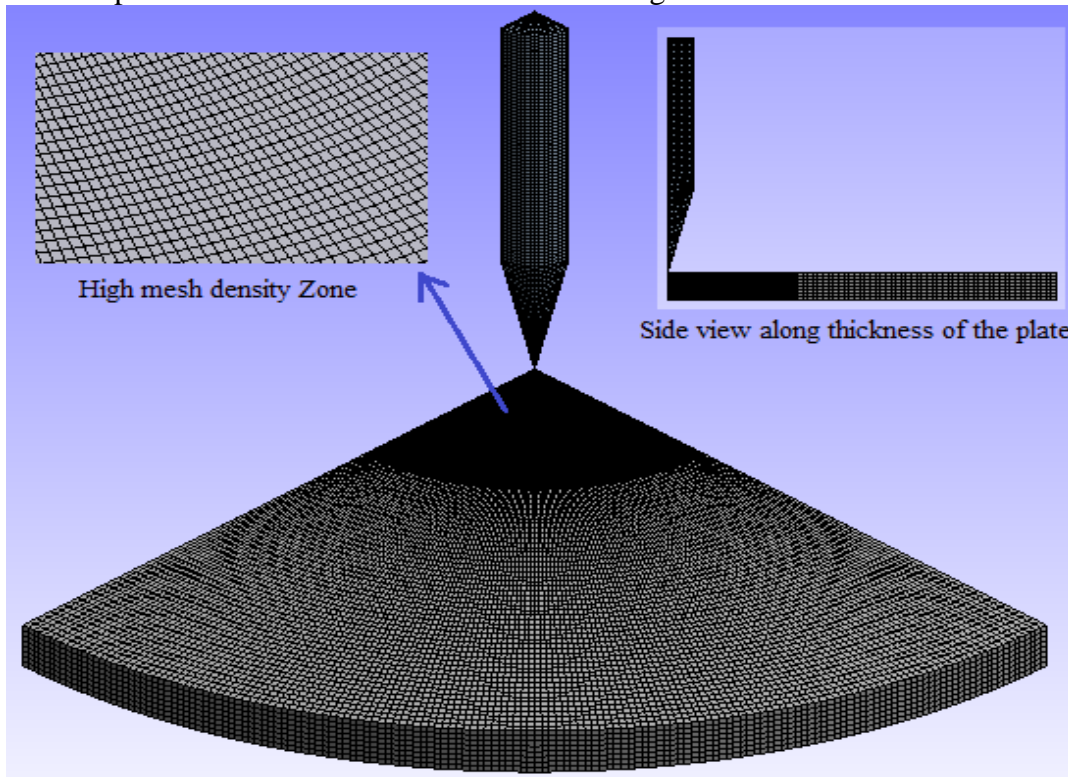


Figure 2 Isometric view of mesh model of the plate and conical ( $30^\circ$ ) projectile

#### 4. RESULTS AND DISCUSSION

The failure modes of steel plate obtained by different conical projectile (varying cone angles starting from  $30^\circ$  to  $180^\circ$ ) are discussed in this section. It is observed that the target plate deform by ductile hole enlargement for lower value of cone angle. For medium cone angle plugging is observed in target plate. Shear plugging is observed in case of higher cone angle. Similar results were reported by Borvik et al. [2] and Arias et al. [4] in their work on blunt projectile and conical

projectile. Equivalent plastic strain contours of the target plate for conical projectile of different cone angles are shown in Fig. 3.

EQUIVALENT PLASTIC STRAIN CONTOURS

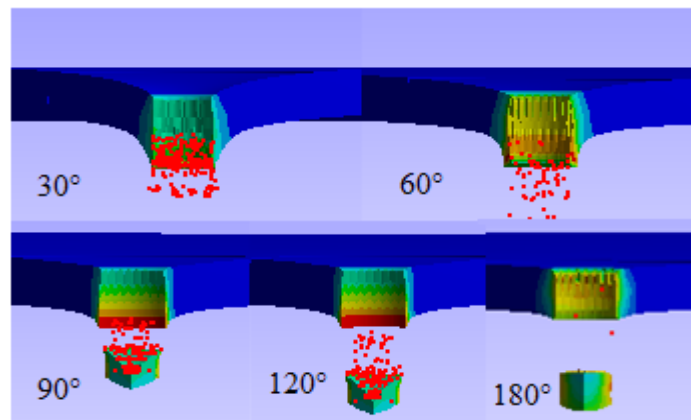


Figure 3 Failure mode obtained in target plate (axisymmetric region) at 500 m/s for different cone angle

Analysis was also conducted for different impact velocity for each cone angle of the projectile and residual velocity was calculated. The variation in residual velocity has been shown in Fig. 4. It was observed that the residual velocity of projectiles significantly depends on the cone angle of the projectile. The result shows that the residual velocity increases with increase in cone angle at low impact velocity. But residual velocity decrease with increase in cone angle at high impact velocity. This behaviour is found due to energy used towards the deformation of plate.

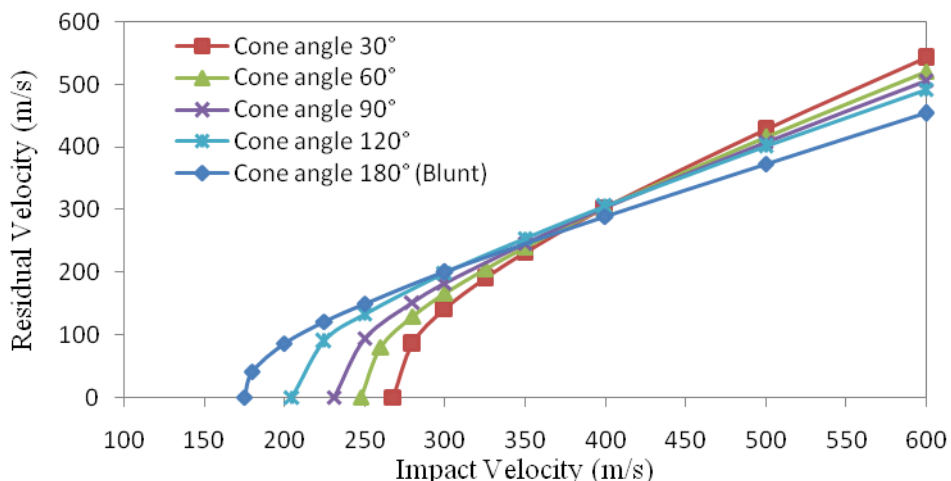


Figure 4 Residual velocities of projectiles at different impact velocity

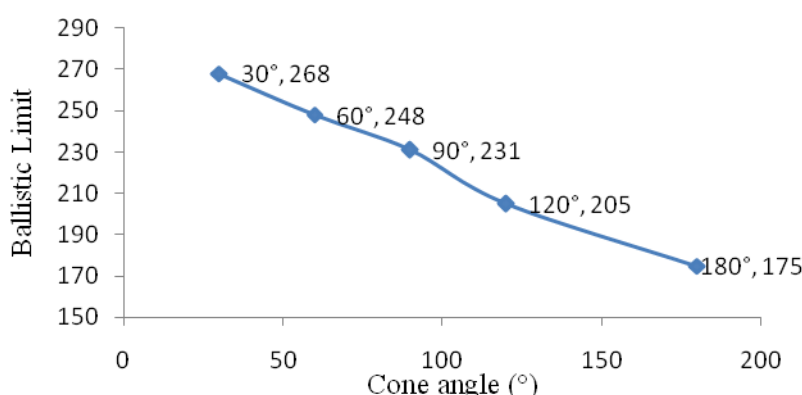


Figure 5 Ballistic limit of different projectiles

The ballistic limit were calculated for each cone angle and is plotted in Fig. 5. The curve shows that ballistic limit is the function of cone angle and decreases as cone angle increase. The ballistic limit is minimum for  $180^\circ$  cone angle i.e. blunt projectile.

The energy used towards the plastic deformation of plate during impact was calculated from the difference of kinetic energy of projectile before and after impact. The energy used for the perforation significantly depends on the cone angle as well as impact velocity of projectile. The variation in the energy with respect to cone angle is shown in Fig. 6.

During the impact of projectile with smaller cone angle the change in energy used for perforation of plate with impact velocity is more or less same. However with projectile of larger cone angle, increase in impact velocity results into increase in energy used for deformation. The energy found maximum for blunt projectile (cone angle  $180^\circ$ ) at high impact velocity.

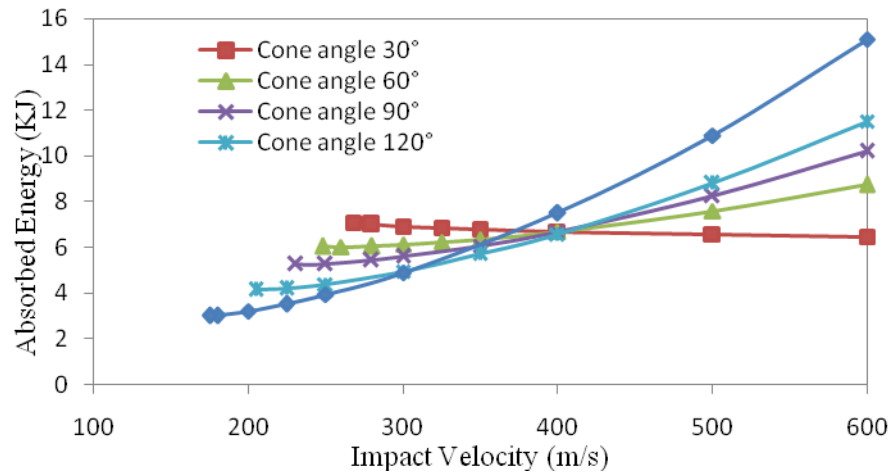


Figure 6 Energy used by plate at different impact velocity

The numerical results of residual velocity obtained in this work for blunt projectile (cone angle  $180^\circ$ ) have been compared with experimental results reported by Borvik et al. [2] and shown in Fig. 7. The figure shows that the numerical results are closely matching with the experimental results.

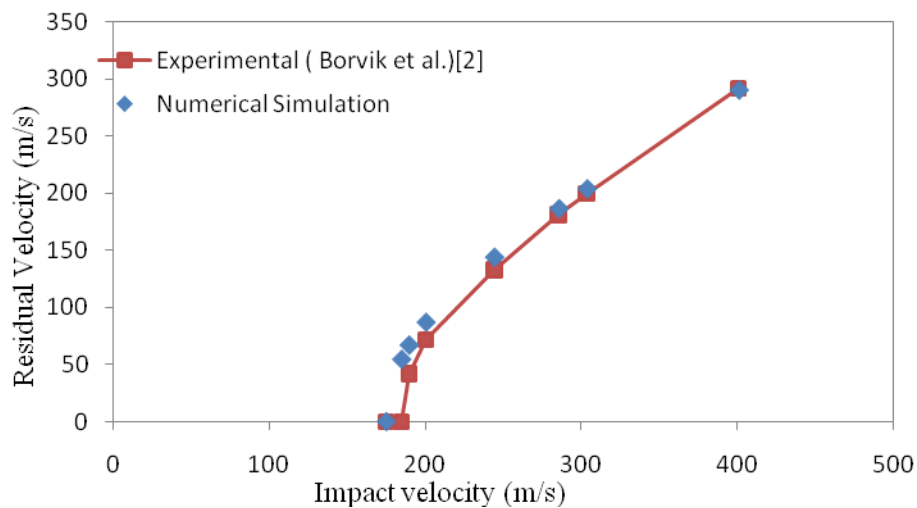


Figure 7 Comparison of experimental and numerical results for  $180^\circ$  cone angle (blunt) projectile

## 5. CONCLUSIONS

The work included numerical studies for the influence of cone angle of conical projectile during the impact on plates to study failure modes, residual velocity, ballistic limit and absorbed energy.

In this analysis different failure modes were observed depending upon cone angle of projectile. As the cone angle increases, failure mode shift to shear plugging from ductile hole enlargement. Ballistic limit also depends upon the cone angle and found minimum for higher cone angle (180°). At high impact velocity the energy used towards the deformation of plate is higher for larger cone angle projectiles. The residual velocity curves are affected by the projectile cone angle and impact velocity. The cone angle as well as impact velocity are responsible for deformation behaviour and failure modes.

## 6. REFERENCES

- [1] Carlucci, D. E. and Jacobson, S. S., (2008). Penetration and Perforation. *Ballistics: Theory and Design of Guns and Ammunition*, CRC Press: 310-315.
- [2] Borvik, T., Langseth, M., Hoperstad, O. S. and Malo, K. A., (2002). Perforation of 12 mm thick steel plates by 20 mm diameter projectiles with flat, hemispherical and conical noses Part I: Experimental study. *International journal of impact engineering*, 27, 19-35.
- [3] Zukas, J.A. and Scheffler, D.R., (2000). Practical aspects of numerical simulations of dynamic events: effects of meshing. *International Journal of Impact Engineering*, 24, 925-945.
- [4] Arias, A., Rodriguez-Martinez, J. A. and Rusinek, A., (2008). Numerical simulations of impact behaviour of thin steel plates subjected to cylindrical, conical and hemispherical non-deformable projectiles. *Engineering fractures mechanics*, 75(6), 1635-1656.
- [5] Gupta, N. K., Iqbal, M. A. and Sekhen, G. S., (2007). Effect of Projectile Nose Shape, Impact Velocity & Target Thickness on deformation of Aluminium Plate. *International Journal of Solids & Structures*, 44, 3411–3439.
- [6] Woodward, R. L., (1984). The interrelation of failure modes observed in the penetration of metallic targets. *International Journal of Impact Engineering* 2(2), 121–129.
- [7] Wilkins, M. L., (1978). Mechanics of penetration and perforation. *International Journal of Engineering Sciences*, 16, 793–807
- [8] Borvik, T., Langseth, M. and Hoperstad, O. S., (2002). Perforation of 12mm thick steel plates by 20mm diameter projectiles with flat, hemispherical and conical noses Part II: numerical simulations. *International journal of impact engineering*, 27, 37–64
- [9] Ansys mechanical user's guide, (2013). SAS IP , Inc
- [10] Johnson, G. R. and Cook, W. H., (1985). Fracture characteristics of three metals subjected to various strains, strain rates, temperatures and pressures. *International Journal of Engng Fracture Mechanics*, 21(1), 31-48
- [11] Johnson, G. R. and Cook, W. H., (1983). A constitutive model and data for metals subjected to large strains, high strain rates and high temperatures. *Proceedings of Seventh International Symposium on Ballistics*, The Hague, The Netherlands
- [12] Borvik, T., Langseth, M., Hopperstad, O. S. and Malo, K. A., (1999). Ballistic penetration of steel plates. *International Journal of Impact Engineering*, 22 (9–10), 855–887
- [13] PTC University, Introduction to Creo elements/Pro 5.0-Fundamentals